

A day-ahead scheduling model of power systems incorporating multiple tidal range power stations

Tong Zhang, Nicolas Hanousek, Meysam Qadrdan, *Senior Member, IEEE*, Reza Ahmadian

Abstract—With the global trend to exploit more renewable energy sources, tidal range energy has been gaining more attention recently. This power generation technology is expected to reduce the share of fossil fuels and provide flexibility to the power system. With a pioneering tidal range generation project just granted in Wales and more proposals planned in Great Britain, it is important to study how the incorporation of multiple tidal range power stations will affect power system operation. In this paper, the role of tidal range energy generation in the future Great Britain power system is investigated based on a day-ahead scheduling model of power system incorporating multiple tidal range power stations. In the proposed model, tidal range power stations situated at different sites operate flexibly and in coordination, supporting the power system to reach the minimum operating cost. A case study based on the Great Britain electricity transmission system in 2030 with one tidal barrage and one tidal lagoon was investigated. The results showed that the coordination of flexible tidal range power stations can reduce the power system's operating cost. Furthermore, the energy-storage feature of tidal range power stations can act as a stable source of flexibility in the power system.

Index Terms—Flexibility, MILP, Operation cost reduction, Power system scheduling, Tidal range energy.

NOMENCLATURE

Index collections

$\mathcal{I}_k^{\text{GEN}}$	Index collection of generation units at Bus k .
$\mathcal{I}_l^{\text{line}+}$	Index of the starting bus of Line l .
$\mathcal{I}_l^{\text{line}-}$	Index of the terminal bus of Line l .
$\mathcal{I}_k^{\text{PV}}$	Index collection of PV plants at Bus k .
$\mathcal{I}_i^{\text{SL}}$	Index collection of sluice gates in the i th tidal range power station.
$\mathcal{I}_i^{\text{TB}}$	Index collection of turbines in the i th tidal range power station.
\mathcal{I}_k^{W}	Index collection of wind plants located at Bus k .
\mathcal{S}^{bus}	Index collection of buses in power system.
\mathcal{S}^{GEN}	Index collection of generation units.
\mathcal{S}^{GT}	Index collection of gas-fired generation units.
\mathcal{S}^{IM}	Index collection of power import nodes.
\mathcal{S}^{LD}	Index collection of load nodes in power system.
$\mathcal{S}^{\text{line}}$	Index collection of lines in power system.
\mathcal{S}^{NU}	Index collection of nuclear power plants.
$\mathcal{S}^{\text{ORES}}$	Index collection of power plants supported by other types of RES.
\mathcal{S}^{PV}	Index collection of PV plants.
\mathcal{S}^{TR}	Index collection of tidal range power station.

\mathcal{S}^{W}	Index collection of wind plants.
\mathcal{T}	Index collection of time periods.

Parameters & Definitions

A_m^{SL}	Cross-sectional flow area of the m th sluice gate (m^2).
A_m^{TB}	Cross-sectional flow area of the m th turbine (m^2).
A_i^{TR}	Impounded area of the i th TRPS (m^2).
c_i^{NU}	The power output of the i th nuclear power plant (MW).
c_i^{ORES}	The power output of the i th power plant supported by other types of RES (MW).
c^{SL}	Discharge coefficient of sluice gates.
c^{TB}	Discharge coefficient of turbines.
C_i^{E}	Price of power generation at the i th generation unit (£/MWh).
C^{IM}	Price of power import (£/MWh).
C^{LS}	Price of load shedding (£/MWh).
C_i^{SU}	Start-up cost of the i th generation unit (£).
g	Gravitational acceleration (m/s^2).
$h_i^{\text{in-initial}}$	The inside water level at beginning time period of the operation (m).
H^{start}	Minimum head difference to activate turbines in a tidal range power station.
K^{SL}	Fitted coefficient used to calculate $Q_{m,t}^{\text{SL-single}}$.
K^{TB}	Fitted coefficient used to calculate $Q_{m,t}^{\text{TB-single}}$.
$L_i^{\text{min-off}}$	Minimum off time length of the i th CCGT (h).
$L_i^{\text{min-on}}$	Minimum on time length of the i th CCGT (h).
$P_i^{\text{PV-fcst}}$	Power output forecast of the i th PV plant (MW).
$P_i^{\text{W-fcst}}$	Power output forecast of the i th wind plant (MW).
$\overline{P}_i^{\text{GT}}, \underline{P}_i^{\text{GT}}$	Maximum/Minimum generation capacity of the i th CCGT (MW).
$\overline{P}_i^{\text{IM}}$	Maximum limit of power import of Bus i (MW).
$\overline{P}_{i,t}^{\text{LS}}$	Maximum limit of load shedding of Bus i at time t (MW).
$\overline{P}_m^{\text{TB-single}}$	Maximum generation capacity of the m th turbine in a TRPS (MW).
\overline{PF}_l	Maximum power transmission on Line l (MW).
$PL_{i,t}$	Power demand of i th load node at time t (MW).
R_t^{PS}	Total spinning reserve demand of the power system (MW/h).
RD_i, RU_i	Spinning-down/Spinning-up ramp rate of the i th generation unit (MW/h).
SD_i, SU_i	Shut-down/Start-up rate of the i th generation unit (MW/h).

Tong Zhang, Nicolas Hanousek, Meysam Qadrdan (Corresponding author) and Reza Ahmadian are with School of Engineering, Cardiff University, Cardiff, UK (e-mails: ZhangT44@cardiff.ac.uk; HanousekN@cardiff.ac.uk; QadrdanM@cardiff.ac.uk; AhmadianR@cardiff.ac.uk).

u_i^{10} The initial on/off status of the i th generation unit.
 x_l Reactance of Line l (Ω).
 ΔT Length of each time step (h).
 $\alpha^{P^{TB}}, \beta^{P^{TB}}$ Constants used in $P^{TB\text{-single}}$ calculation.
 $\alpha^{Q^{TB}}, \beta^{Q^{TB}}$ Constants used in $Q^{TB\text{-single}}$ calculation.

Variables

$E_{i,t}^{TR}$ The energy production of the i th TRPS at time t (MWh).
 F^{total} Total cost of power system operation (\mathcal{L}).
 $h_{i,t}^{\text{in}}, h_{i,t}^{\text{out}}$ Water level inside/outside the i th TRPS at time t (m).
 $H_{i,t}$ Head difference between inside and outside the i th TRPS at time t (m).
 $P_{i,t}^{\text{GEN}}$ The power generation of the i th generation unit at time t (MW).
 $P_{i,t}^{\text{GT}}$ The power generation of the i th CCGT at time t (MW).
 $P_{i,t}^{\text{IM}}$ The power import of Bus i at time t (MW).
 $P_{i,t}^{\text{LS}}$ The amount of load shedding of Bus i at time t (MW).
 $P_{i,t}^{\text{NU}}$ The power generation of the i th nuclear power plant at time t (MW).
 $P_{i,t}^{\text{ORES}}$ The power generation of the i th power plant supported by other types of RES at time t (MW).
 $P_{i,t}^{\text{W}}$ The power generation of the i th wind plant at time t (MW).
 $P_{i,t}^{\text{W-curt}}$ The power output curtailment of the i th wind plant at time t (MW).
 $P_{i,t}^{\text{PV}}$ The power generation of the i th PV plant at time t (MW).
 $P_{i,t}^{\text{PV-curt}}$ The power output curtailment of the i th PV plant at time t (MW).
 $P_{i,t}^{\text{LS}}$ The load shedding at Bus i at time t (MW).
 $P_{m,t}^{\text{TB-single}}$ The power output of the m th turbine in a TRPS at time t (MW).
 $P_{i,t}^{\text{TR}}$ The power output of the i th TRPS at time t (MW).
 $PF_{l,t}$ The power transmission on Line l at time t (MW).
 $Q_{i,t}^{\text{SL}}$ The total amount of water flowing through the i th TRPS's sluice gates at time t (m^3/s).
 $Q_{m,t}^{\text{SL-single}}$ The amount of water flowing through the m th sluice gate at time t (m^3/s).
 $Q_{i,t}^{\text{TB}}$ The total amount of water flowing through the i th TRPS's turbines at time t (m^3/s).
 $Q_{m,t}^{\text{TBf-single}}$ The amount of water flowing through the m th turbine during the filling phase at time t (m^3/s).
 $Q_{m,t}^{\text{TBg-single}}$ The amount of water flowing through the m th turbine during the generating phase at time t (m^3/s).
 $Q_{i,t}^{\text{TR}}$ The total amount of water flowing through the i th TRPS at time t (m^3/s).
 $R_{i,t}^{\text{D}}, R_{i,t}^{\text{U}}$ The spinning-down/spinning-up reserve capacity of the i th generation unit at time t (MW).
 $u_{i,t}$ Binary variable showing the on/off status of the i th generation unit at time t .
 $X_{i,t}^{\text{off}}, X_{i,t}^{\text{on}}$ The time length that the i th generation unit has

been kept off/on at time t .
 $y_{i,t}, z_{i,t}$ Binary variable showing the start-up/shut-down of the i th generation unit at time t .
 $\delta_{i,t}^{\text{filling}}$ Binary variable indicating whether the TRPS is at the filling phase.
 $\delta_{i,t}^{\text{head}}$ Binary variable indicating whether $H_{i,t}$ is positive or not.
 $\delta_{i,t}^{\text{gen}}$ Binary variable indicating whether the TRPS is at the generating phase.
 $\delta_{m,t}^{\text{on-fill}}$ Binary variable indicating whether the m th turbine is filling or not during a filling phase at time t .
 $\delta_{m,t}^{\text{on-gen}}$ Binary variable indicating whether the m th turbine is generating or not during a generating phase at time t .
 $\epsilon_{m,t}^{P^{TB\text{-gen}}}$ Auxiliary variable as the replacement of the product of $\delta_{m,t}^{\text{on}}$ and $P_{m,t}^{\text{TB-single}}$ (MW).
 $\theta_{i,t}$ The voltage angle of Bus i at time t (rad).

I. INTRODUCTION

A. Background

DRIVEN by the fossil fuel depletion and the net-zero goal, the proportion of renewable energy is growing year by year. In the past decades, a considerable amount of focus has been put on wind and solar energy. On the contrary, marine energy is much less developed. In 2020, the worldwide gross electricity generation of marine energy was around 1 TWh, less than 0.005% of the total generation, while wind and solar energy taking 6% and 3% respectively [1]. As a branch of marine energy, tidal range energy has been known for its high predictability as it is driven by the gravitation pulls of the moon and the sun, and the mean absolute errors of forecast tides are usually less than 20 cm [2]. Tidal range structures also have a longer life span of generation facility compared with wind and solar energy [3]. In addition, a tidal range power station (TRPS) is capable of operating in a flexible way by adjusting its generation output either through curtailing power from a subset of the operating turbines or shifting the generation time window, which entitles itself to provide flexibility to the power system and help the system accommodate more intermittent renewable energy.

The tidal range power stations are of two forms: tidal barrage and tidal lagoon, both of which are designed to convert the gravitational potential energy of water into electricity. The tidal barrage is long established and currently there are two operating tidal barrage projects: the Rance Tidal Barrage (the world's first tidal range power station) and Sihwa Lake Tidal Power Station. The tidal lagoon is still a novel tidal range generation technology. The first proposal to develop a tidal lagoon was Swansea Bay Tidal Lagoon project [4], which was later rejected due to the concerns of high cost. In November 2021, another proposal for developing a tidal lagoon at Swansea Bay, as a part of the larger project named Blue Eden Project, was announced. This indicates the great confidence in tidal range technology from the industry. As a country with the second highest tidal range resources in the world [5], the role and value of tidal range energy in

decarbonising the UK's energy supply need to be investigated further.

B. Literature review

There have been many investigations around the tidal range generation. There are studies on the tidal range resources, such as the approximation of extractable tidal energy around the Great Britain coastline [6] or from a single tidal range proposal [7]. The impacts of tidal range generation have been evaluated, including the hydrodynamic interference [8], the effect on nature conservation [9], the eutrophication risk [10]. The positive contributions of tidal range energy have also been assessed, including contribution to the medium-term variability of the future UK's energy mix [5] and carbon emission reduction [11].

Various simulation models have been developed to examine the hydrodynamics and generation output of tidal range power stations, including a 0-D model developed according to the continuity principle [12] and various 2-D models such as DIVAST-2DU [13], ADCIRC [14], TELEMAC [15] and Thetis [16]. Whereas 2-D models solve forms of the Navier-Stokes equations to simulate the full physical behaviour of the unsteady and turbulent water flows in the region, 0-D models assume the water is distributed uniformly and depict the hydrodynamics based on water flow continuity by algebraic equations, which are far less computationally demanding [17]. Based on these models, the optimisation of tidal range schemes has been explored as well. An operational optimisation of a tidal barrage using ebb-only generation was proposed in [18], adjusting the energy generation by varying the starting heads instead of physical changes to the barrage. A gradient-based optimisation method for the TRPS was developed in [16], with consideration of the hydrodynamic response to the marine structures. Genetic Algorithm was also employed in the optimal design of tidal range schemes with the goal to maximise the power output [17], [19]. Apart from maximising energy generation, the maximisation of the tidal range scheme's economic value was also investigated, such as the optimised operation of a TRPS by exploiting the flexible timing of generation in [20]. Furthermore, the investigation of the operation of a TRPS fleet was conducted based on the flexibility provided by individual tidal lagoons and the longer cumulative generation duration caused by tidal phase difference. In [21], the feasibility of a continuous tidal energy supply by controlling prospective TRPSs in an cooperative system was evaluated. In [22], an income-incentive optimisation model to maximise the collective income of seven prospective tidal lagoons in the UK was proposed.

However, the aforementioned studies predominantly focused on the operation of tidal range power stations without explicitly considering their bidirectional interactions with the wider power systems they are connected to. For instance, the operation of tidal range power stations were investigated to achieve maximum electricity generation or revenue from selling electricity to the wholesale market considering a given price profile [?]. Although, such studies provide useful insights into the economic viability of tidal range schemes and

their capability to operate flexibly, they do not capture the whole system value of tidal range power stations in terms of supporting the short term balancing of electricity supply and demand in the presence of variable renewable generation technologies. To the authors' best of knowledge, so far, there hasn't been any study on the scheduling of power systems incorporating flexible operation of multiple tidal range power stations. Yet, key questions remained unanswered are: (a) how should TRPSs operational characteristics be incorporated and formulated in the Unit Commitment and Economic Dispatch problem of a power system? and (b) what are 'whole-system' impacts of multiple TRPSs in terms of reduction in emission, renewable curtailment and operational cost of a power system?

C. Contributions

To address the identified research questions, this paper develops a day-ahead scheduling model of power system incorporating multiple tidal range schemes to investigate the role and value of tidal range energy in a future GB power system. The operational characteristics of TRPSs were formulated as linearised constraints based on a 0-D model and included in a day-ahead optimal scheduling model of the power system. The operation of the GB power system with multiple TRPSs was investigated under different supply/demand scenarios to quantify the impacts of the coordinated operation of TRPSs. More specifically, the contributions of this paper are:

- 1) A model of tidal range energy generation was formulated to depict the hydraulics-power relationship in a TRPS. This model was built based on a 0-D model derived from the hydrodynamic data and converted into a mixed integer linear form to reduce computation complexity. The model captures key operational characteristics of a TRPS and its capability to operate flexibly.
- 2) The day-ahead scheduling optimisation of power system incorporating multiple tidal range power stations was proposed for the first time. This model enabled quantifying the 'whole-system' value of operating TRPSs flexibly. Two TRPSs at different locations on the west coast of GB were considered to operate flexibly and in coordination with each other to support the operation of the power system. The proposed optimisation model was tested under different operating scenarios to reveal the contributions of tidal range power stations.

The remainder of this paper is organised as follows. Section 2 gives a brief introduction to tidal range energy generation, including the TRPS's structure, operation schemes, and the potential benefits of tidal range scheme coordination. Section 3 presents the modelling of TRPS operation and the day-ahead scheduling model of power system with multiple tidal range schemes. Section 4 introduces the case study, with Section 5 presenting the result and data analysis. Section 6 concludes this paper.

II. INTRODUCTION TO TIDAL RANGE ENERGY GENERATION

A. The structure of a tidal range power station

A tidal range power station is a man-made impoundment that utilizes the tides to generate electric power. The impound-

ment can be built either as a barrage (spanning an estuary) or a lagoon (either coastally attached, or entirely offshore) [23]. The turbines and sluice gates are constructed through the walls to control the inflow/outflow of water. As shown in Fig. 1, the TRPS impoundment is separated from the open sea by the structure walls, which creates a head difference across the structure. When the head difference reaches a predetermined level, the turbine housings are opened and the water flows through the turbines, propelling the turbines to rotate and convert the kinetic energy into electric power. Between generation periods, the TRPS can adjust the status of turbines and sluice gates to hold the water level inside the lagoon or quickly fill/empty the lagoon as required.

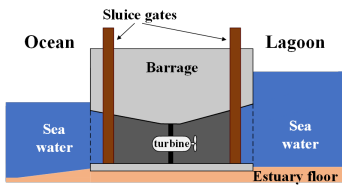


Fig. 1. The structure of a tidal barrage/lagoon's wall

B. The operating schemes of a tidal range power station

There are three key modes of operation used by a TRPS, one-way generation (ebb-only generation and flood-only generation) and two-way generation. In this paper, the tidal range power stations in the proposed model employ the ebb-only generation and two-way generation, demonstrated in Fig. 2.

For the ebb-only/flood-only generation, the TRPS generates power during ebb/flood cycle and rests during the other cycle. The operation of a TRPS here consists of three phases: holding, filling and generating. The TRPS stays in the filling phase during the majority of the flood cycle, as both turbines and sluice gates are open (no power output by turbines) to let the water quickly fill the basin. When the water levels across the impounding structure reach the same in the ebb cycle, the holding phase begins and both the turbines and sluice gates are closed to hold the water inside the basin. As the outside water level drops due to the ebbing tide, the head difference increases. When the head difference is higher than the starting requirement (H^{start}), the TRPS enters the generating phase, as the turbines are activated (with closed sluice gates) and start generating power. When the head difference is too low for the efficient generation of turbines (H^{end}), the TRPS re-enters the holding phase and starts filling shortly after it. To further increase the head difference that will be achieved for the generation phase, the turbines are also operated as pumps between filling/sluicing and holding in some operational configurations.

For the two-way generation, the TRPS generates in both ebb and flood cycles and the turbines generate in more time periods than the one-way generation. Starting from the generating phase in the flood cycle, turbines keep generating while sea water flows into the basin. When the head difference is lower than the requirement H^{end} , the TRPS enters a filling phase when both turbines and sluice gates are open. In this study, the TRPS adopts the parallel sluicing mode and the turbines are generating during the filling phases too. After the water

levels of both sides reach the same, the holding phase begins as both turbines and sluice gates are closed to create a larger head difference for efficient turbine generation, followed by the second generating phase where water is released from the basin through turbines. The TRPS goes through the same holding-generating-filling process in both flood and ebb cycles.

In any operation mode, the TRPS could work in a flexible generation scheme, adjusting the generation output by changing the value of H^{start}/H^{end} , or curtailing power from a subset of turbines during generating phases. In this paper, the TRPSs generate electricity flexibly by changing the number of generating turbines and shifting the generation window (H^{start} and H^{end} stay fixed). On the contrary, the TRPS could work in a fixed generation scheme, which is predetermined to reach the TRPS's maximal generation capacity. The generation scheme and the number of active turbines stayed fixed during the whole operation, without any response to the fluctuation of system load and RES generation.

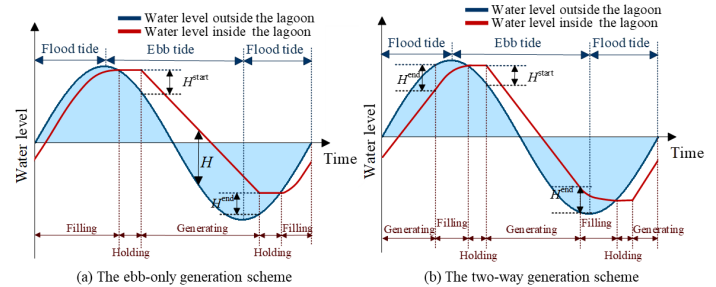


Fig. 2. The generation schemes of tidal range power stations

C. The potential of tidal range generation coordination

There are several sites around the UK coastline to be considered for tidal range proposals, including the Bristol Channel, Liverpool, and Morecambe bays, the Solway Firth, the Wash, the Duddon, the Wyre, and the Conway [24]. Although most of the sites have semidiurnal tide cycles, there might be phase differences between different locations. Taking the West Somerset and Mersey Barrage as an example, there is a five-hour delay in the tidal elevations (as shown in Fig. 3), which may cause a difference in the generation timing of the tidal power stations located in these two areas. Accumulating these asynchronous generation outputs, the fleet of TRPS will have a longer time window of continuous power supply, which enables tidal range energy to support the power system for more time periods.

Unlike wind/solar power plants, TRPS has an "energy-storage" feature due to its ability to adjust power output by controlling the operating status of turbines/sluices. This flexible generation scheme allows the tidal barrage/lagoon to hold water inside the lagoon and release it during other time periods. Therefore, the basin can store a certain amount of potential energy during low power demand and supply it to the system as demanded, similar to the battery energy storage system. However, the head difference across the impoundment varies with the flood/ebb, which leads to a fluctuating capacity of energy stored in the tidal lagoon and the varying flexibility that can be provided to the power system. Combining the longer time window of continuous power supply and the

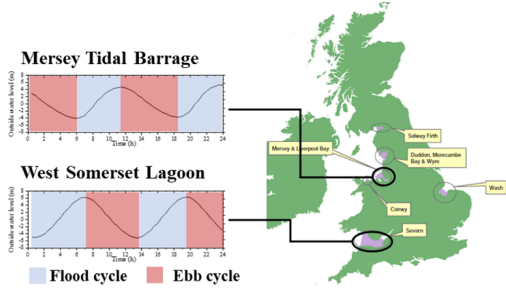


Fig. 3. The potential sites of tidal range power stations in the GB with tidal data on 02/01/2018

time-varying flexibility provided by tidal range generation, the coordination of TRPS will make positive contributions to power system while facing greater computation complexity during optimisation.

III. DAY-AHEAD SCHEDULING OPTIMISATION OF POWER SYSTEMS WITH TIDAL RANGE SCHEMES

To investigate the role of tidal range generation in the power system's operation, the day-ahead scheduling optimisation of power system incorporating multiple tidal range schemes was formulated. The tidal range power stations are assumed to be connected to one or multiple buses in the power system. In the same manner as conventional coal-fired or gas-fired power stations, the operating plan of the tidal range power stations is decided before the real-time market. The proposed optimisation model is therefore modelled as below.

A. Objective Function

The objective function is to minimise the total operation cost of the power system, which includes the fuel cost, the start-up cost of generation units, the cost of power import and the cost of power load shedding, written as below:

$$\begin{aligned} \min F^{\text{total}} = & \sum_{t \in \mathcal{T}} \left\{ \sum_{i \in \mathcal{S}^{\text{GEN}}} (C_i^E P_{i,t}^{\text{GEN}}) \right\} + \sum_{t \in \mathcal{T}} \left\{ \sum_{i \in \mathcal{S}^{\text{GEN}}} (C_i^{\text{SU}} y_{i,t}) \right\} \\ & + \sum_{t \in \mathcal{T}} \left\{ \sum_{i \in \mathcal{S}^{\text{bus}}} (C^{\text{IM}} P_{i,t}^{\text{IM}}) \right\} + \sum_{t \in \mathcal{T}} \left\{ \sum_{I \in \mathcal{S}^{\text{LD}}} (C^{\text{LS}} P_{I,t}^{\text{LS}}) \right\} \quad (1) \end{aligned}$$

B. Constraints

1) *Power system constraints:* The total amount of power generation should meet the power demand, presented as:

$$\begin{aligned} \sum_{i \in \mathcal{S}^{\text{GEN}}} P_{i,t}^{\text{GEN}} + \sum_{i \in \mathcal{S}^{\text{IM}}} P_{i,t}^{\text{IM}} + \sum_{i \in \mathcal{S}^{\text{W}}} P_{i,t}^{\text{W}} + \sum_{i \in \mathcal{S}^{\text{PV}}} P_{i,t}^{\text{PV}} + \sum_{i \in \mathcal{S}^{\text{TR}}} P_{i,t}^{\text{TR}} \\ = \sum_{i \in \mathcal{S}^{\text{LD}}} (P_{I,t} - P_{I,t}^{\text{LS}}), \quad \forall t \in \mathcal{T} \quad (2) \end{aligned}$$

In (2), P^{GEN} includes generation from combined cycle gas turbines (CCGTs), biomass power plant, nuclear power plants and other types of renewable power plants.

The constraint of power flow along transmission lines is:

$$PF_{l,t} = \frac{\theta_{i,t} - \theta_{j,t}}{x_l}, \quad \forall l \in \mathcal{S}^{\text{line}}, i \in \mathcal{I}_l^{\text{line}+}, j \in \mathcal{I}_l^{\text{line}-}, \forall t \in \mathcal{T} \quad (3)$$

The limit of power flow is:

$$-\overline{PF}_l \leq PF_{l,t} \leq \overline{PF}_l, \quad \forall l \in \mathcal{S}^{\text{line}}, \forall t \in \mathcal{T} \quad (4)$$

For CCGTs, the constraints on the change of on/off states of CCGT units are built using three sets of binary variables ($u_{i,t}$, $y_{i,t}$ and $z_{i,t}$) to represent the on/off status, start-up and shut-down action, written as:

$$y_{i,t} + z_{i,t} \leq 1, \quad \forall i \in \mathcal{S}^{\text{GT}}, \forall t \in \mathcal{T} \quad (5)$$

$$y_{i,t} - z_{i,t} = \begin{cases} u_{i,t} - u_i^0, & t = 1 \\ u_{i,t} - u_{i,t-1}, & \text{else} \end{cases}, \quad \forall i \in \mathcal{S}^{\text{GT}}, \forall t \in \mathcal{T} \quad (6)$$

The limit on CCGT's power generation capacity is:

$$u_{i,t} \underline{P}_{i,t}^{\text{GT}} \leq P_{i,t}^{\text{GT}} \leq u_{i,t} \overline{P}_{i,t}^{\text{GT}}, \quad \forall i \in \mathcal{S}^{\text{GT}}, \forall t \in \mathcal{T} \quad (7)$$

The limits on CCGT's generation ramp rate are:

$$P_{i,t}^{\text{GT}} - P_{i,t-1}^{\text{GT}} \leq (1 - y_{i,t})RU_i + y_{i,t}SU_i, \quad \forall i \in \mathcal{S}^{\text{GT}}, \forall t \in \mathcal{T} \quad (8)$$

$$P_{i,t-1}^{\text{GT}} - P_{i,t}^{\text{GT}} \leq (1 - z_{i,t})RD_i + z_{i,t}SD_i, \quad \forall i \in \mathcal{S}^{\text{GT}}, \forall t \in \mathcal{T} \quad (9)$$

The limits on CCGT's spinning-up/down reserve capacity are:

$$R_{i,t}^{\text{U}} \leq \overline{P}_{i,t}^{\text{GT}} - P_{i,t}^{\text{GT}}, \quad \forall i \in \mathcal{S}^{\text{GT}}, \forall t \in \mathcal{T} \quad (10)$$

$$R_{i,t}^{\text{D}} \leq P_{i,t}^{\text{GT}} - u_{i,t} \underline{P}_{i,t}^{\text{GT}}, \quad \forall i \in \mathcal{S}^{\text{GT}}, \forall t \in \mathcal{T} \quad (11)$$

The min-on/off time constraints are:

$$(X_{i,t-1}^{\text{on}} - L_i^{\text{min-on}})(u_{i,t-1} - u_{i,t}) \geq 0, \quad \forall i \in \mathcal{S}^{\text{GT}}, t \geq 1 \quad (12)$$

$$(X_{i,t-1}^{\text{off}} - L_i^{\text{min-off}})(u_{i,t-1} - u_{i,t}) \geq 0, \quad \forall i \in \mathcal{S}^{\text{GT}}, t \geq 1 \quad (13)$$

For the whole power system, the total capacity of spinning reserve should meet the system requirement:

$$\sum_{i \in \mathcal{S}^{\text{GEN}}} R_{i,t}^{\text{U}} \geq R_t^{\text{PS}}, \quad \forall t \in \mathcal{T} \quad (14)$$

The constraints on the wind/PV generation units are:

$$P_{i,t}^{\text{W}} = P_{i,t}^{\text{W-fcst}} - P_{i,t}^{\text{W-curt}}, \quad \forall i \in \mathcal{S}^{\text{W}}, \forall t \in \mathcal{T} \quad (15)$$

$$P_{i,t}^{\text{PV}} = P_{i,t}^{\text{PV-fcst}} - P_{i,t}^{\text{PV-curt}}, \quad \forall i \in \mathcal{S}^{\text{PV}}, \forall t \in \mathcal{T} \quad (16)$$

The limits on wind/PV curtailment are:

$$0 \leq P_{i,t}^{\text{W-curt}} \leq P_{i,t}^{\text{W-fcst}}, \quad \forall i \in \mathcal{S}^{\text{W}}, \forall t \in \mathcal{T} \quad (17)$$

$$0 \leq P_{i,t}^{\text{PV-curt}} \leq P_{i,t}^{\text{PV-fcst}}, \quad \forall i \in \mathcal{S}^{\text{PV}}, \forall t \in \mathcal{T} \quad (18)$$

The power outputs of nuclear power plants and other renewable power plants are assumed to be constant throughout the day:

$$P_{i,t}^{\text{NU}} = c_i^{\text{NU}}, \quad \forall i \in \mathcal{S}^{\text{NU}}, \forall t \in \mathcal{T} \quad (19)$$

$$P_{i,t}^{\text{ORES}} = c_i^{\text{ORES}}, \quad \forall i \in \mathcal{S}^{\text{NU}}, \forall t \in \mathcal{T} \quad (20)$$

The limit on the amount of power import is:

$$0 \leq P_{i,t}^{\text{IM}} \leq \overline{P}_i^{\text{IM}}, \quad \forall i \in \mathcal{S}^{\text{IM}}, \forall t \in \mathcal{T} \quad (21)$$

The limit on load shedding is:

$$0 \leq P_{i,t}^{\text{LS}} \leq \overline{P}_{i,t}^{\text{LS}}, \quad \forall i \in \mathcal{S}^{\text{LD}}, \forall t \in \mathcal{T} \quad (22)$$

2) *Tidal range power station constraints:* Both 0-D models and 2-D models have been used to depict the hydrodynamics of TRPSs. In general, 2-D models consider the water dynamics in two directions while 0-D models only consider the water continuity. The 0-D models have been found to produce higher yield estimates than 2-D models (by up to 12% in the case of [19]), however the relative reduction in computational cost has been accepted to outweigh this deviation, leading to the use of 0-D becoming standard. In this model, the hydrodynamics of a TRPS is represented by a 0-D model [6]. The relationship between hydraulics and generation is described by the equations below.

The water level inside the basin is determined by the water level in the previous time period and the amount of inflow/outflow through the structure walls:

$$h_{i,t}^{\text{in}} = \begin{cases} h_i^{\text{in-initial}}, & t = 0 \\ h_{i,t-1}^{\text{in}} - \frac{Q_{i,t}^{\text{TR}}}{A_i^{\text{TR}}} \Delta T, & \forall t \in \mathcal{T}, \forall i \in \mathcal{S}^{\text{TR}} \end{cases} \quad (23)$$

The head difference is decided by the water level inside and outside the basin:

$$H_{i,t} = h_{i,t}^{\text{in}} - h_{i,t}^{\text{out}}, \quad \forall i \in \mathcal{S}^{\text{TR}}, \forall t \in \mathcal{T} \quad (24)$$

The amount of inflow/outflow is the sum of water flowing through the sluice gates and turbines:

$$Q_{i,t}^{\text{TR}} = (2\delta_{i,t}^{\text{head}} - 1) \cdot Q_{i,t}^{\text{SL}} + (2\delta_{i,t}^{\text{head}} - 1) \cdot Q_{i,t}^{\text{TB}}, \quad \forall i \in \mathcal{S}^{\text{TR}}, \forall t \in \mathcal{T} \quad (25)$$

In (25), $\delta_{i,t}^{\text{head}}$ is a binary variable indicating the direction of water flow across the impoundment (when $H_{i,t} > 0$, $\delta_{i,t}^{\text{head}} = 1$ as the water outflows the basin; otherwise $\delta_{i,t}^{\text{head}} = 0$). $Q_{i,t}^{\text{SL}}$ and $Q_{i,t}^{\text{TB}}$ represent the total amount of water flowing through the sluice gates and turbines, respectively. When the water is flowing out from the basin, $Q_{i,t}^{\text{TR}}$ is positive, and vice versa.

The sluice gates are open during the filling phase only. The total amount of inflow/outflow through sluice gates is calculated by the equation below:

$$Q_{i,t}^{\text{SL}} = \delta_{i,t}^{\text{filling}} \sum_{m \in \mathcal{I}_i^{\text{SL}}} Q_{m,t}^{\text{SL-single}}, \quad \forall i \in \mathcal{S}^{\text{TR}}, \forall t \in \mathcal{T} \quad (26)$$

In (26), $\delta_{i,t}^{\text{filling}}$ is a binary variable indicating whether the i th tidal range power station is at the filling phase ($\delta_{i,t}^{\text{filling}} = 1$ during the filling phase; otherwise $\delta_{i,t}^{\text{filling}} = 0$).

When the sluice gates are open, the water flowing through an individual sluice gate can be calculated using $H_{i,t}$:

$$Q_{m,t}^{\text{SL-single}} = c^{\text{SL}} A_m^{\text{SL}} \sqrt{2g|H_{i,t}|}, \quad \forall m \in \mathcal{I}_i^{\text{SL}}, \forall i \in \mathcal{S}^{\text{TR}}, \forall t \in \mathcal{T} \quad (27)$$

which could be styled into a linear form to reduce computation complexity:

$$Q_{m,t}^{\text{SL-single}} = K^{\text{SL}} A_m^{\text{SL}} |H_{i,t}|, \quad \forall m \in \mathcal{I}_i^{\text{SL}}, \forall i \in \mathcal{S}^{\text{TR}}, \forall t \in \mathcal{T} \quad (28)$$

As for turbines, the total amount of water flow and power output are the sum of water flow/power output of activated turbines, which can be calculated using the equations below:

$$Q_{i,t}^{\text{TB}} = \sum_{m \in \mathcal{I}_i^{\text{TB}}} \delta_{m,t}^{\text{on-gen}} Q_{m,t}^{\text{TB-single}} + \sum_{m \in \mathcal{I}_i^{\text{TB}}} \delta_{m,t}^{\text{on-fill}} Q_{m,t}^{\text{TBf-single}}, \quad \forall i \in \mathcal{S}^{\text{TR}}, \forall t \in \mathcal{T} \quad (29)$$

$$P_{i,t}^{\text{TR}} = \sum_{m \in \mathcal{I}_i^{\text{TB}}} (\delta_{m,t}^{\text{on-gen}} + \delta_{m,t}^{\text{on-fill}}) \cdot P_{m,t}^{\text{TB-single}}, \quad \forall i \in \mathcal{S}^{\text{TR}}, \forall t \in \mathcal{T} \quad (30)$$

In (29) and (30), $\delta_{m,t}^{\text{on-gen}}$ and $\delta_{m,t}^{\text{on-fill}}$ are binary variables indicating the on/off status of the m th turbine during the generating/filling phase of the i th TRPS (when the m th turbine is generating, $\delta_{m,t}^{\text{on-gen}}$ or $\delta_{m,t}^{\text{on-fill}}$ are equal to 1; otherwise $\delta_{m,t}^{\text{on-gen}}$ and $\delta_{m,t}^{\text{on-fill}}$ are equal to 0).

For each turbine, the relationship between the unit speed, unit discharge, and power output could be found in literature [25], which could be transferred into a hill chart with water flow and power output plotted against the head difference [26]. Taking a 20-MW bulb turbine as an example, a hill chart depicting the head-flow and head-power relationship could be obtained by scaling the 20 MW bulb turbine's data, as shown in Fig. 4.

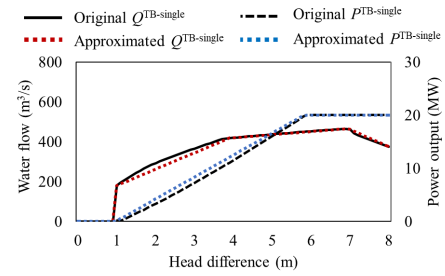


Fig. 4. The hill chart of 20 MW bulb turbine

The water discharge and power output curves could be fitted by linear segments, which are written as:

$$Q_{m,t}^{\text{TB-single}} = \begin{cases} 0, & |H_{i,t}| < H^{\text{start}} \\ \alpha_1^{\text{QTB}} |H_{i,t}| + \beta_1^{\text{QTB}}, & H^{\text{start}} \leq |H_{i,t}| \leq 3.9 \\ \alpha_2^{\text{QTB}} |H_{i,t}| + \beta_2^{\text{QTB}}, & 3.9 \leq |H_{i,t}| \leq 7 \\ \alpha_3^{\text{QTB}} |H_{i,t}| + \beta_3^{\text{QTB}}, & 7 \leq |H_{i,t}| \leq 10 \end{cases} \quad \forall m \in \mathcal{I}_i^{\text{TB}}, \forall i \in \mathcal{S}^{\text{TR}}, \forall t \in \mathcal{T} \quad (31)$$

$$P_{m,t}^{\text{TB-single}} = \begin{cases} \alpha_1^{\text{PTB}} |H_{i,t}|, & |H_{i,t}| < H^{\text{start}} \\ \alpha_2^{\text{PTB}} |H_{i,t}| + \beta_2^{\text{PTB}}, & H^{\text{start}} \leq |H_{i,t}| \leq 7 \\ \beta_3^{\text{PTB}}, & |H_{i,t}| > 7 \end{cases} \quad \forall m \in \mathcal{I}_i^{\text{TB}}, \forall i \in \mathcal{S}^{\text{TR}}, \forall t \in \mathcal{T} \quad (32)$$

In (31) and (32), α and β are constants used in the linear equations, which could be estimated using the hill chart. For a TRPS adopting the ebb-only generation scheme, the turbines stay inactive during the whole filling phase, so the α_1^{PTB} stays zero. For a TRPS adopting the two-way generation scheme, there is still a small amount of power produced during the filling phase, so the α_1^{PTB} is a non-zero constant. (31) and (32) were formulated as piecewise linear constraints in the proposed linear model.

During the filling phase, the water flowing through an individual turbine could be calculated using $H_{i,t}$:

$$Q_{m,t}^{\text{TBf-single}} = c^{\text{TB}} A_m^{\text{TB}} \sqrt{2g|H_{i,t}|}, \quad \forall m \in \mathcal{I}_i^{\text{TB}}, \forall i \in \mathcal{S}^{\text{TR}}, \forall t \in \mathcal{T} \quad (33)$$

which could be approximated as a linear equation as well:

$$Q_{m,t}^{\text{TBf-single}} = K^{\text{TB}} A_m^{\text{TB}} |H_{i,t}|, \quad \forall m \in \mathcal{I}_i^{\text{TB}}, \forall i \in \mathcal{S}^{\text{TR}}, \forall t \in \mathcal{T} \quad (34)$$

The constraint of energy production is:

$$E_{i,t}^{\text{TR}} = P_{i,t}^{\text{TR}} \cdot \Delta T, \quad \forall i \in \mathcal{S}^{\text{TR}}, \forall t \in \mathcal{T} \quad (35)$$

Equations (25), (26), (29), and (30) contain the products of a binary variable and a continuous variable, which causes higher computational complexity. These nonlinear terms were relaxed to a linear form. Taking the product of $\delta_{m,t}^{\text{on-gen}}$ and $P_{i,t}^{\text{TB-single}}$ in (30) as an example, an auxiliary variable $\epsilon_{m,t}^{\text{P}^{\text{TB-gen}}}$ ($\epsilon_{m,t}^{\text{P}^{\text{TB-gen}}} \geq 0$) was used as a replacement to calculate the m th turbine's power output at time t , and the original constraints were rewritten as:

$$\epsilon_{m,t}^{\text{P}^{\text{TB-gen}}} = \delta_{m,t}^{\text{on-gen}} P_{m,t}^{\text{TB-single}} \quad (36)$$

$$\epsilon_{m,t}^{\text{P}^{\text{TB-gen}}} \leq \delta_{m,t}^{\text{on-gen}} \cdot \bar{P}_m^{\text{TB-single}} \quad (37)$$

$$\epsilon_{m,t}^{\text{P}^{\text{TB-gen}}} \leq P_{m,t}^{\text{TB-single}} \quad (38)$$

$$\epsilon_{m,t}^{\text{P}^{\text{TB-gen}}} \geq P_{m,t}^{\text{TB-single}} - (1 - \delta_{m,t}^{\text{on-gen}}) \cdot \bar{P}_m^{\text{TB-single}} \quad (39)$$

IV. CASE STUDY

In this paper, a test system combining the GB 30-bus electricity transmission system (ETS) and two tidal range power stations was used for the case study. Description of the test system and cases are given as below.

A. Test system description

The GB electricity transmission system consists of 30 buses, 53 branches and 130 generation units, which was formulated based on the model from [27], [28]. To investigate the role of TRPS in the future, the ETS was modelled under one of the future energy scenarios (consumer transformation) given by National Grid [29]. It is supported by various energy sources, including CCGTs, nuclear power plants, biomass power plants, wind power plants, solar power plants, other renewable power plants, and interconnectors (the total capacity of each generation technology is given in Tab. I).

For tidal range energy, two prospective TRPS sites are involved: the Mersey Tidal Barrage (MTB) and the West Somerset Lagoon (WSL), which are connected to the GB ETS via Bus Deeside and Bus Melksham respectively. The generation mode and parameters of these two TRPSs are given in Tab. II.

TABLE I

THE INSTALLED CAPACITY OF EACH GENERATION TECHNOLOGY							
Generation technology	CCGT	Nuclear	Biomass	Wind	Solar	Other RES	Import
Capacity (GW)	31.57	4.57	6.31	58.93	29.04	7.52	18.65

TABLE II

TIDAL RANGE POWER STATION SPECIFICATIONS		
TRPS	MTB	WSL
Generation mode	Ebb-only	Two-way
Numbers of turbine	28	125
Turbine diameter (m)	8	7.2
Turbine capacity (MW)	25	20
Total sluice area (m ²)	2592	20000
Basin area (km ²)	52	82

To evaluate the impact of TRPS comprehensively, the proposed scheduling model was run with different levels of wind/PV penetration and power demand. Four supply/demand profiles were used in the test runs, which are noted as highDemand-highRES, highDemand-lowRES, lowDemand-highRES and lowDemand-lowRES. The range of total power demand is between 23.6 GW and 62.4 GW. The range of total power supply from wind/solar is from 0 GW to 8.7 GW, and from 5.2 GW to 39.0 GW, respectively.

The energy stored in a TRPS is determined by the tidal range, which might be higher or lower during the spring/neap tide days. As the tidal period follows a lunar day (24 hours and 50 minutes), the timing of highest/lowest tide moves through the day on a 28-day cycle. The combination of different timings and ranges of tide variation in two TRPSs generates many tide profiles, making the outcome of optimisation model vary on different days. The proposed optimal scheduling model contains 51369 continuous variables and 16560 integer variables (including 16368 binary variables). The computation of a 24-hour optimisation usually takes two to eight hours (the computation burden may vary with different tide data and system profiles). To avoid the great computation burden brought by running the proposed day-ahead scheduling model of a longer term, a representative day was adopted in the case study. This representative day was identified as the smallest combined absolute deviation from the mean power output of TRPSs, using the pre-determined optimum fixed head configurations from [19]. The supply/demand profiles, and the outside water levels of TRPSs are presented in Fig. 5.

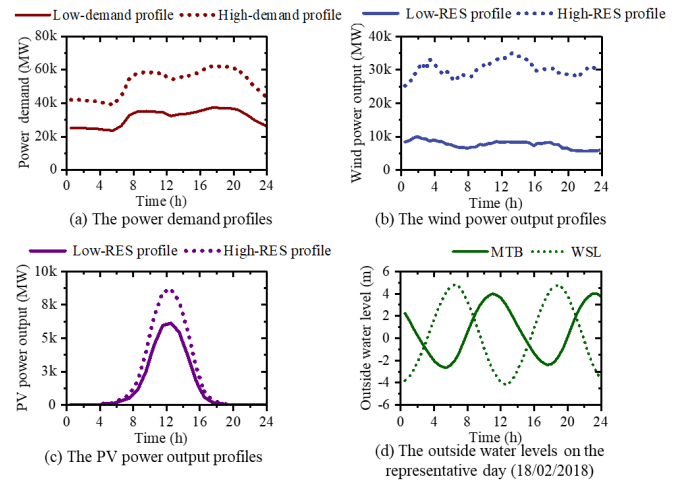


Fig. 5. The power system setting and tide data used in the test runs

The scheduling horizon of the proposed day-ahead scheduling model is 24 hours with a 30-minute time step. The test run was performed in Python with Gurobi Solver on a laptop powered by an Intel Core i7 processor and 8 GB RAM.

B. Case description

Three operating scenarios were studied to analyse the impact of TRPS incorporation:

- 1) *P*Only: Power system without TRPS incorporation;

- 2) *PS+MaxTR*: Power system with the MTB and the WSL working individually under a fixed generation scheme to reach maximum energy generation;
- 3) *PS+FlexTR*: Power system with the MTB and the WSL working in coordination with a flexible generation scheme.

V. RESULT AND DISCUSSION

A. Validation of the linear 0-D tidal range generation model

To ensure the accuracy of the simplified TRPS model used in this paper, a model validation procedure was carried out by comparing simulation results by the linear 0-D TRPS model (Linear-0D) proposed in Section III-B with the result by another published 0-D model (Benchmark-0D) [19]. In both models, all turbines were set to generate when $H > H^{start}$ and be switched off when $H > H^{end}$. The details of model settings are given in Tab. III. For the rest of model settings, both models used the similar mode and parameters as presented in Tab. II.

TABLE III
MODEL SETTINGS OF BENCH-0D AND LINEAR-0D MODELS

TRPS	Time step	A^{TR}	H^{start}	H^{end}	Ramp time
Bench-0D	5 min	Varying	1 m	1 m	20 min
Linear-0D	30 min	Fixed	1 m	1 m	0 min

The comparison of simulation results in Mersey Tidal Barrage and West Somerset Lagoon is presented in Fig. 6 and Fig. 7. The patterns of water level elevation and the timing of each generating phase in the Linear-0D results are almost identical to the Benchmark-0D results. For Mersey Tidal Barrage, the normalised root mean square deviations (NRMSDs) of inner water level, energy production, and the water flow via turbines/sluice gates are 10.6%, 7.5%, 9.5% and 13.4%. As a longer time step was used in the Linear-0D model, when the MTB switches from the filling phase to the holding phase, the open/closed status of turbines and sluice gates might be different from Bench-0D, causing the deviations in water inflow/outflow and head difference. For West Somerset Lagoon, the NRMSDs of inner water level, energy production, and the water flow via turbines/sluice gates are 2.9%, 6.7%, 22.5% and 6.5%, which mainly come from the deviation of $Q^{TB-single}$ and $Q^{SL-single}$ linearisation.

It should be noted that this study aims to investigate the impact of TRPS incorporation on the power system operation, rather than creating an accurate simulation model of TRPS. So the main purpose of model validation is to ensure the day-ahead scheduling model could obtain practical solutions. Considering the linearisation in turbine characteristic curves, a longer time step and the fixed basin area used in the Linear-0D model, the computation deviation is within an acceptable range.

B. Optimal day-ahead scheduling of power system with multiple tidal range schemes

1) *Cost reduction and change in energy supply mix*: To show the contribution of coordinated TRPSs to the operation cost reduction, the total operation cost of power system under

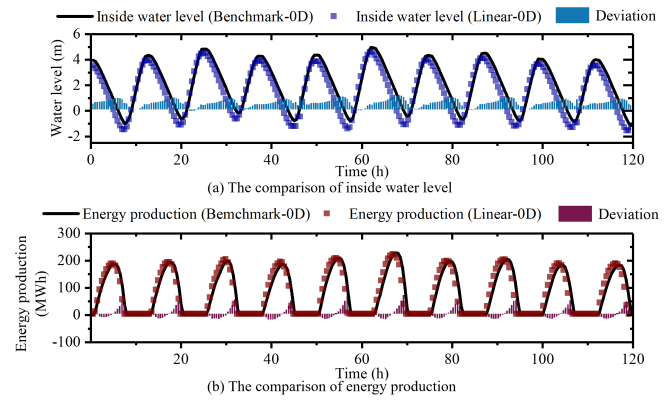


Fig. 6. The result comparison between the linear-0D model and the benchmark-0D model in Mersey Tidal Barrage

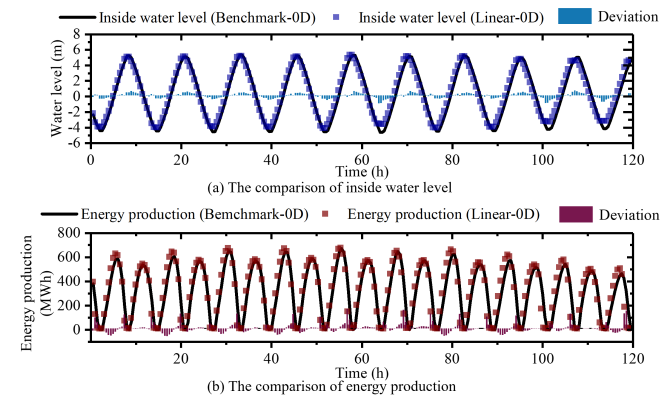


Fig. 7. The result comparison between the linear-0D model and the benchmark-0D model in West Somerset Lagoon

four supply/demand profiles are given in Tab. IV. Although the operation cost varies under different supply/demand levels, incorporating tidal range energy into the power system always can reduce the total operation cost. Furthermore, compared with result of TRPSs working in the fixed generation scheme, the coordination of flexible-generation TRPSs could offer more cost reduction, which accounts for 3.01%, 1.69%, 1.18% and 2.67% of the total operation cost respectively.

TABLE IV
COMPARISON OF TOTAL OPERATION COST (£ MILLION)

Supply/demand profiles	<i>PSonly</i>	<i>PS+MaxTR</i>	<i>PS+FlexTR</i>
highDemand-highRES	44.57	43.28	43.23
highDemand-lowRES	98.73	97.11	97.06
lowDemand-highRES	14.32	14.20	14.15
lowDemand-lowRES	49.52	48.26	48.20

The cost reduction is greatly impacted by the level of power demand and RES penetration, as the proportion of each type of energy and the generation time window of each power plants are different. Fig. 8 and Fig. 9 provide more details about the cost and energy supply mix in the three operating scenarios. The cost reduction mainly comes from the fuel cost cut-down, as the TRPSs replace the energy production of some thermal generation units (CCGTs and biomass power plants). The coordination of TRPSs has the least cost reduction contribution under the lowDemand-highRES profile, which

is only £ 128,529. This is because the power output from wind/PV power plant is already higher than the total power demand during most of the day, so the system only needs a small amount of energy supply from the biomass power plant from 19:00 to 21:00, without any energy production by CCGT. Hence the TRPS could only reduce very limited amount of fuel cost of the biomass power plants. Contrarily, the incorporation of TRPSs has the highest cost-reduction effect (£ 1,663,920) during the high-demand and low-RES profile. As can be seen from Fig. 9(b), the substantial gap between the demand and RES power output exceeds the installed capacity of all thermal generation units so the energy from power interconnectors and TRPSs is greatly needed all the day. To reduce fuel cost and power import cost, both MTB and WSL are working in the generation schemes that are almost the same as the fixed generation schemes to maximise their energy production. Under the highDemand-highRES profile and the lowDemand-lowRES profile, the incorporation of TRPSs reduces £ 1,339,424 and £ 1,324,003 respectively. During these two profiles, the gap between power demand and RES power output is around 20% to 65% of the total installed capacity of thermal generation units, and the CCGT and biomass power plants support the power system with more frequent start-ups and shutdowns. As two TRPSs actively engage in the operation of power system, with shifting in generation time window and adjustment of active turbine number, a new balance between the fuel cost, the start-up cost, and power import cost is found to reach a lower operation cost. This could explain the fluctuation of cost on thermal generation units' start-up and power import.

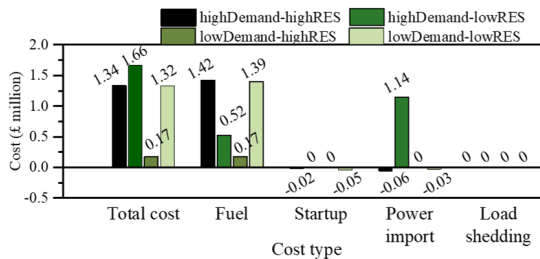


Fig. 8. The cost reduction of coordinated TRPSs in the *PS+FlexTR* scenario
 2) *The flexible generation schemes of TRPSs*: To show how the coordination of multiple TRPSs contributes to the operation of power system, the detailed generation schemes of TRPSs (both *PS+MaxTR* and *PS+FlexTR*) under the highDemand-highRES profile are presented in Fig. 10, Fig. 11 and Tab. V.

TABLE V
 PEAK ENERGY PRODUCTION AND GENERATION DURATION COMPARISON

Model	<i>PS+MaxTR</i>		<i>PS+FlexTR</i>	
	MTB	WSL	MTB	WSL
Peak power output (MW)	283.62	1,396.40	451.94	1398.90
Duration of generation (h)	8.5	14	8	17

When working in the fixed generation schemes, MTB generates from 3:00 to 7:00 and from 15:00 to 19:00, with an eight-hour time gap between each generation time window. The WSL has four generation cycles during one day, with a time gap of around 2.5 hours. When working in the flexible generation schemes, both the timing and the amount of energy generation are adjusted to reach the goal of total operation cost minimisation. During time 2:30 to 3:00, the MTB starts

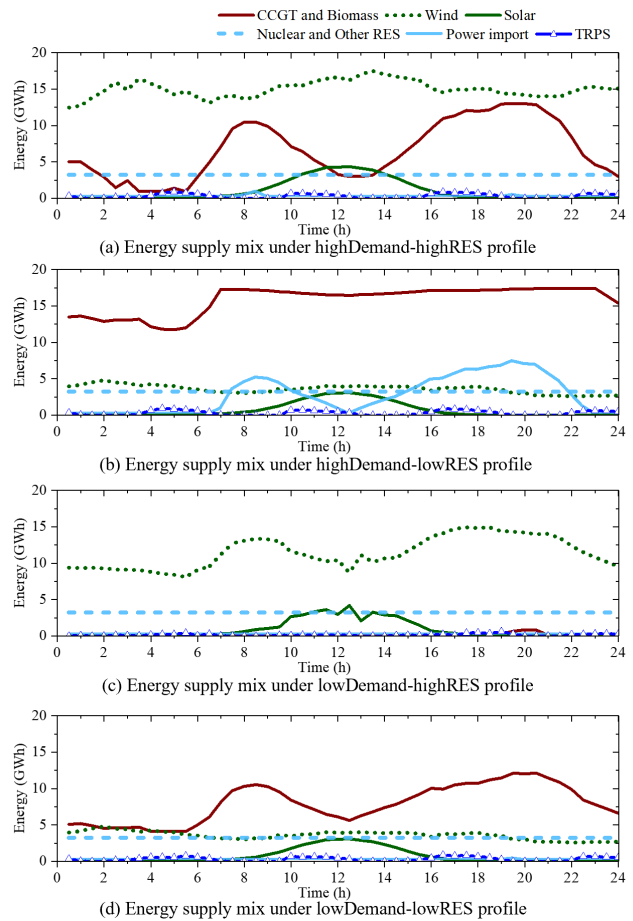


Fig. 9. Energy supply mix comparison under four supply/demand profiles

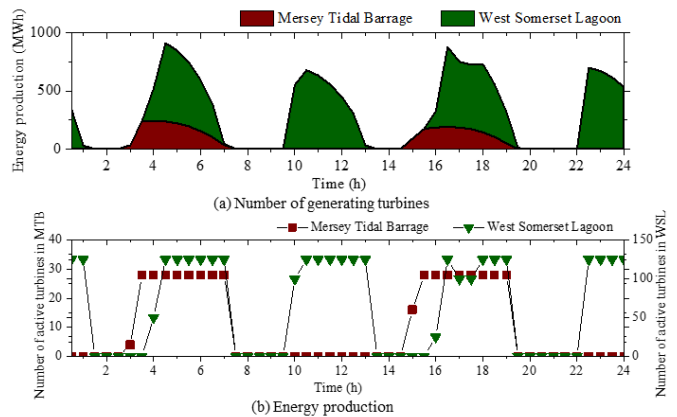


Fig. 10. The *PS+MaxTR* generation schemes of TRPSs under the highDemand-highRES profile

its generation cycle half an hour earlier, with all turbines on rather than only four in the fixed generation schemes. This is to cover the energy produced by some of the thermal power units. As the system power demand decreases from 2:00 to 5:00, the MTB shifts its generation time window to earlier periods when energy is more needed. The WSL has a longer generation window in the *PS+FlexTR* scenario, as the duration of each generation cycle is longer. Around 7:00, the system is experiencing growth in demand, the WSL

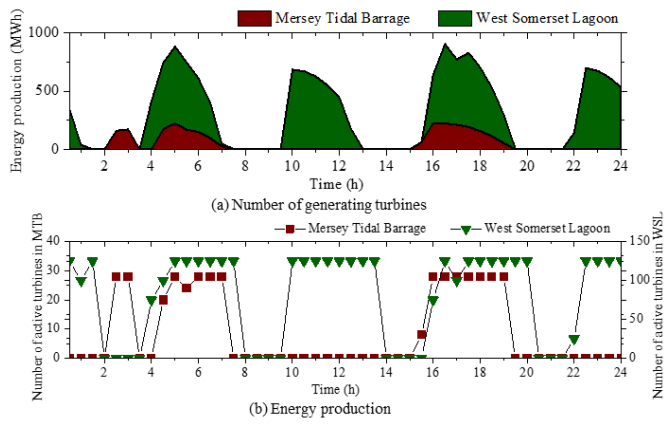


Fig. 11. The *PS+FlexTR* generation schemes of TRPSs under the highDemand-highRES profile

postpones the termination of the first generation cycle to save as much fuel consumption as possible. Between 19:00 and 22:00, although system demand is decreasing, the wind power generation is relatively low compared with 18:00 and 23:00, which requires a relatively high energy production from the thermal generation units. To reduce the fuel cost, the WSL prolongs its third generation cycle and starts the fourth generation cycle earlier, narrowing the time gap to only one hour and replacing more energy production of the thermal power units. This shows that TRPSs are capable of shifting the timing of generation and adjusting the amount of energy production in response to the power system demand and the power output fluctuation of wind/PV power plants.

3) *Energy stored by TRPS*: The potential energy stored by a TRPS could be transferred into electricity if needed, which could be regarded as a storage-like energy source that is supported by TRPSs. However, due to the fluctuation of water levels both inside and outside, the energy stored in TRPSs varies during the day. The stacked area charts showing the energy stored by MTB and WSL under four demand/supply profiles are presented in Fig. 12.

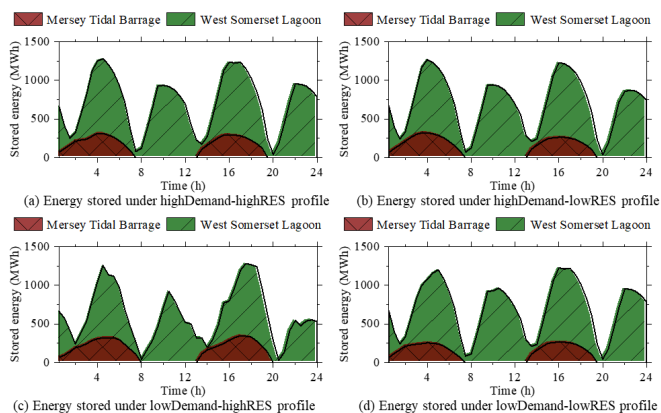


Fig. 12. The energy stored by TRPSs under four supply demand profiles

The energy stored by TRPSs was calculated based on the power production corresponding to the varying head difference, which could be found in the turbine hill charts. It shows the same increase/decrease pattern as the energy production

in the previous section, as both are determined by the head difference. The MTB is available to provide energy during most of the ebb cycles (from midnight to 7:00, and from 13:00 to 19:30). The WSL is available to provide energy almost all the time. This is because the WSL is working in a two-way generation scheme with the parallel sluicing mode. When the head difference is lower than H^{end} during the filling phase, the turbines are still available to generate a small amount of power. Accumulating the energy stored by MTB and WSL, the coordinated TRPSs could continuously supply energy to the power system.

There are still differences in the peaks and valleys between the subplots in Fig. 12, which is mainly due to the difference in the TRPS generation schemes. Under the lowDemand-highRES profile, the TRPS energy storage seems to have a more evenly slope in the increase and decrease, and stays in the peaks for a shorter time. This is because the tidal range energy is less needed during the lowDemand-highRES profile, as the head difference in basins doesn't need to stay at high levels to maintain high power output for a relatively long time, the head difference drops quickly after reaching the peak. During the other supply/demand profiles, the patterns are quite similar, with small deviations in the values of peaks and valleys only. This shows that the coordination of multiple TRPSs can store a certain amount of energy and is capable of providing continuous energy support to the power system.

VI. CONCLUSION

To investigate the impact of coordination of multiple tidal range schemes in the GB power system, a day-ahead scheduling model of power system combining the Mersey Tidal Barrage and the West Somerset Lagoon has been proposed in this paper. The operation of tidal range power stations used in the optimisation model is modelled based on a simplified linear 0-D model, which has been validated. To present the contribution of TRPSs during different days, test runs have been carried out under four different supply/demand profiles on a representative day.

The result shows that the incorporation of multiple tidal range schemes can effectively reduce the total operation cost of power system, mainly the fuel cost. The amount of cost reduction is greatly affected by the power demand and renewable energy penetration level. During most supply/demand profiles, the coordinated TRPSs could provide a daily cost reduction of more than £ 1.3 million. It is also demonstrated that to reach the cost reduction goal, each tidal range power station could adjust its power output according to the demand and supply conditions, by shifting the timing of each generation cycle and adjusting the number of active turbines. The energy stored by TRPSs is also quantified. The amount of energy stored varies during the day as it's determined by the head difference which changes with the flood/ebb tides and different generation schemes of TRPSs. Accumulating the energy storage in Mersey Tidal Barrage and West Somerset Lagoon, the coordinated tidal range structures could provide a power system with a continuous energy supply.

For the future work, the flexibility provision by a fleet of tidal range schemes will be evaluated and the tidal range

energy's contribution in the power system optimisation with stochastic renewable energy integration will be studied. To comprehensively investigate the potential benefit of tidal range energy, the participation of a tidal range power station in the grid service market will be explored as well.

ACKNOWLEDGMENTS

This research was supported by the UK Engineering and Physical Sciences Research Council (EPSRC) (grant numbers: EP/W027879/1 and EP/L016214/1). Meysam Qadrdan would like to also acknowledge EPSRC for supporting him via an Innovation Fellowship (grant number: EP/S001492/1). For the purpose of open access, the authors have applied a Creative Commons Attribution (CC BY) license to any accepted manuscript version arising.

REFERENCES

- [1] International Energy Agency, *World Energy Outlook 2021*, 2021.
- [2] G. D. Egbert and R. D. Ray, "Tidal prediction," *Journal of Marine Research*, vol. 75, no. 3, pp. 189–237, 2017.
- [3] C. Hendry, *The Role of Tidal Lagoons*, 2016.
- [4] S. Waters and G. Aggidis, "A world first: Swansea Bay tidal lagoon in review," *Renewable and Sustainable Energy Reviews*, vol. 56, pp. 916–921, 2016.
- [5] G. Todeschini, D. Coles, M. Lewis, I. Popov, A. Angeloudis, I. Fairley, F. Johnson, A. Williams, P. Robins, and I. Masters, "Medium-term variability of the uk's combined tidal energy resource for a net-zero carbon grid," *Energy*, vol. 238, p. 121990, 2022.
- [6] R. Burrows, I. Walkington, N. Yates, T. Hedges, J. Wolf, and J. Holt, "The tidal range energy potential of the west coast of the United Kingdom," *Applied Ocean Research*, vol. 31, no. 4, pp. 229–238, 2009.
- [7] S. Petley and G. Aggidis, "Swansea Bay tidal lagoon annual energy estimation," *Ocean Engineering*, vol. 111, pp. 348–357, 2016.
- [8] A. Angeloudis and R. A. Falconer, "Sensitivity of tidal lagoon and barrage hydrodynamic impacts and energy outputs to operational characteristics," *Renewable Energy*, vol. 114, pp. 337–351, 2017.
- [9] J. S. Pethick, R. K. Morris, and D. H. Evans, "Nature conservation implications of a Severn tidal barrage—a preliminary assessment of geomorphological change," *Journal for Nature Conservation*, vol. 17, no. 4, pp. 183–198, 2009.
- [10] M. Kadiri, H. Zhang, A. Angeloudis, and M. D. Piggott, "Evaluating the eutrophication risk of an artificial tidal lagoon," *Ocean & Coastal Management*, vol. 203, p. 105490, 2021.
- [11] K. Kelly, M. McManus, and G. Hammond, "An energy and carbon life cycle assessment of tidal power case study: The proposed Cardiff–Weston Severn Barrage scheme," *Energy*, vol. 44, no. 1, pp. 692–701, 2012.
- [12] D. Prandle, "Simple theory for designing tidal power schemes," *Advances in water resources*, vol. 7, no. 1, pp. 21–27, 1984.
- [13] B. Lin, J. M. Wicks, R. A. Falconer, and K. Adams, "Integrating 1D and 2D hydrodynamic models for flood simulation," in *Proceedings of the Institution of Civil Engineers-Water Management*, vol. 159, no. 1. Thomas Telford Ltd, 2006, pp. 19–25.
- [14] R. A. Luetlich, J. J. Westerink, N. W. Scheffner *et al.*, "ADCIRC an advanced three-dimensional circulation model for shelves, coasts, and estuaries. Report 1, Theory and methodology of ADCIRC-2DD1 and ADCIRC-3DL," 1992.
- [15] B. Guo, R. Ahmadian, and R. A. Falconer, "Refined hydro-environmental modelling for tidal energy generation: West somerset lagoon case study," *Renewable Energy*, vol. 179, pp. 2104–2123, 2021.
- [16] A. Angeloudis, S. C. Kramer, A. Avdis, and M. D. Piggott, "Optimising tidal range power plant operation," *Applied energy*, vol. 212, pp. 680–690, 2018.
- [17] J. Xue, R. Ahmadian, and O. Jones, "Genetic algorithm in tidal range schemes' optimisation," *Energy*, vol. 200, p. 117496, 2020.
- [18] G. Aggidis and D. Benzon, "Operational optimisation of a tidal barrage across the mersey estuary using 0-D modelling," *Ocean Engineering*, vol. 66, pp. 69–81, 2013.
- [19] J. Xue, R. Ahmadian, O. Jones, and R. A. Falconer, "Design of tidal range energy generation schemes using a genetic algorithm model," *Applied Energy*, vol. 286, p. 116506, 2021.
- [20] F. Harcourt, A. Angeloudis, and M. D. Piggott, "Utilising the flexible generation potential of tidal range power plants to optimise economic value," *Applied Energy*, vol. 237, pp. 873–884, 2019.
- [21] L. Mackie, D. Coles, M. Piggott, and A. Angeloudis, "The potential for tidal range energy systems to provide continuous power a uk case study," *Journal of Marine Science and Engineering*, vol. 8, no. 10, p. 780, 2020.
- [22] L. Mackie, F. Harcourt, A. Angeloudis, and M. D. Piggott, "Income optimisation of a fleet of tidal lagoons," in *Proceedings of the 13th Wave and Tidal Energy Conference, Naples, Italy*, 2019, pp. 1–6.
- [23] S. P. Neill, A. Angeloudis, P. E. Robins, I. Walkington, S. L. Ward, I. Masters, M. J. Lewis, M. Piano, A. Avdis, M. D. Piggott *et al.*, "Tidal range energy resource and optimization—past perspectives and future challenges," *Renewable energy*, vol. 127, pp. 763–778, 2018.
- [24] S. D. Commission, "Research Report 1, UK tidal resource assessment," http://www.sd-commission.org.uk/data/files/publications/TidalPowerUK1-Tidal_resource_assessment.pdf, 2007.
- [25] G. Aggidis and O. Feather, "Tidal range turbines and generation on the Solway Firth," *Renewable energy*, vol. 43, pp. 9–17, 2012.
- [26] R. A. Falconer, J. Xia, B. Lin, and R. Ahmadian, "The Severn Barrage and other tidal energy options: Hydrodynamic and power output modeling," *Science in China Series E: Technological Sciences*, vol. 52, no. 11, pp. 3413–3424, 2009.
- [27] National Grid, "Electricity ten year statement 2014," <https://www.nationalgrid.com/sites/default/files/documents/37790-ETYS202014.pdf>.
- [28] M. Qadrdan, "Data-gb-electricity-network," <https://github.com/MeysamQ/Data-GB-Electricity-network.git>.
- [29] National Grid, "Future energy scenarios 2020 data workbook," <https://www.nationalgrideso.com/document/173806/download>.